

Effects of Ga and Sn Additions on the Creep Strength and Oxidation Resistance of Near- α Ti Alloys



TOMONORI KITASHIMA, YOKO YAMABE-MITARAI, SATOSHI IWASAKI,
and SHUJI KURODA

The effects of Ga and Sn additions, with an almost constant value regarding Al equivalence, on the creep properties and oxidation resistance of the near- α Ti alloy Ti-5Al-4Zr-1Mo were investigated. The creep strain rate increased due to the replacement of Sn with Ga, which was accompanied by an increase in the volume fraction of primary equiaxed α phase. In addition, the replacement of Sn with Ga decreased the activation energy of the steady-state creep rate for the similar volume fraction of the equiaxed α phase. Ga addition improved the oxidation resistance without Ga segregation at the TiO₂/substrate interface, whereas Sn promoted oxide spallation with metallic Sn segregation at the interface. Ga uniformly dissolved into the internal TiO₂ and into the external Al₂O₃ as a result of solid solution formation between Ga₂O₃ and the aforementioned oxides, which suppressed oxide growth. The formation of (GaAl)₂TiO₅ in TiO₂ and Al₂O₃ was also discussed on the basis of the phase relationships in the TiO₂-Al₂O₃-Ga₂O₃ system.

DOI: 10.1007/s11661-016-3748-4

© The Minerals, Metals & Materials Society and ASM International 2016

I. INTRODUCTION

CONVENTIONAL near- α Ti alloys, which are used in high-temperature applications such as jet engines, are strengthened by solid solution and by the formation of precipitates such as intermetallic silicides and the α_2 phase.^[1-4] The addition of α phase stabilizers such as Al, Sn, and Ga is known to enhance the high-temperature strength of α Ti alloys by solid solution.^[5-8] In addition, the formation of α_2 phase with the DO₁₉ structure in near- α alloys increases strength by precipitation strengthening. Al, Sn, and Ga form the DO₁₉ crystal structure in binary systems of Ti-X (X = Al, Sn, Ga), *i.e.*, Ti₃Al in the Ti-Al system, Ti₃Sn in the Ti-Sn system, and Ti₃Ga in the Ti-Ga system, in addition to ternary and multicomponent systems.^[9-13] The interaction between α_2 particles and moving dislocations, such as interactions that lead to particles shearing or bypassing dislocations, depends on the size, distribution, and volume fraction of the particles.^[9] The formation of large amounts of α_2 phase leads to embrittlement. Rosenberg demonstrated that α -Ti alloys in the Ti-Al system tend to order when they contain as little as 5 or 6 wt pct Al and to embrittle when they contain more than 8.5 wt pct Al.^[12] To avoid embrittlement due to the formation of the α_2 phase or ordering in multicomponent Ti alloys, the empirical Al-equivalent

formula given by $\text{Al} + 1/2 \times \text{Ga} + 1/3 \times \text{Sn} + 1/6 \times \text{Zr} + 10 \times \text{O}$ in wt pct, which is associated with the amounts of the α -stabilizing elements, has been used; the empirical Al equivalence should not exceed 9 for practical use.^[12,13] Thus, controlling the amount of such α stabilizers while considering the Al equivalence is essential for enhancing strength while maintaining ductility in near- α Ti alloys.

The volume fraction of α phase in near- α Ti alloys is high, *e.g.*, approximately 95 at. pct at 1073 K (800 °C),^[11] because diffusion in the α -phase with an hcp structure is slower and because deformation is more difficult compared with that in the β -phase with a bcc structure.

The deformation behavior of α -Ti has been previously studied.^[6,14-16] At room temperature and below, Ti slips along $\langle 11\bar{2}0 \rangle$ on $\{10\bar{1}0\}$, (0001), and $\{10\bar{1}1\}$ planes by the motion of $1/3\langle 11\bar{2}0 \rangle$ or along a dislocation.^[14,15] α -Ti also exhibits a number of twinning modes. This twinning is suppressed by an increase in the Al content and is inhibited at high temperatures.^[16] Williams *et al.* demonstrated that solution hardening of Al in Ti and Ti-Al single crystals occurred *via* both prism and basal slip at 300 K and 1000 K (27 °C and 727 °C).^[16] The increase in tensile strength at room temperature due to substitutional concentrations of α -stabilizer solutes was considered to be proportional to the square root of the atomic fraction of solute contents in Ti-Al-Ga-Sn systems.^[6] The Ti-Sn system exhibited the highest tensile strength, followed by Ti-Ga and Ti-Al systems at the same atomic fraction. However, the difference in strength between the Ti-Sn and Ti-Ga systems was one-third of that between the Ti-Ga and Ti-Al systems. The authors demonstrated that the addition of Ga to Ti was more effective than the addition of Sn in increasing

TOMONORI KITASHIMA, Senior Researcher, and YOKO YAMABE-MITARAI, Group Leader, are with the High Temperature Material Design Group, National Institute for Materials Science, 1-2-1, Sengen, Tsukuba, Ibaraki 305-0047, Japan. Contact e-mail: kitashima.tomonori@nims.go.jp SATOSHI IWASAKI, Principal Engineer, and SHUJI KURODA, Engineer, are with the Materials Manufacturing Group, National Institute for Materials Science.

Manuscript submitted April 28, 2016.

Article published online September 19, 2016

the 0.2 pct proof strength and the tensile strengths at room temperature and at 923 K (650 °C) at the same quantity per unit weight.^[17] With respect to creep deformation, Ga addition has been reported to increase the creep strength in disordered α -Ti, which is attributable to electronic and atomic size effects.^[7,18]

As evident in the aforementioned studies, the authors of these studies on the effect of Ga addition primarily focused on the high-temperature strength and creep strength of α and α/α_2 alloys. In this study, the effects of Ga and/or Sn addition on the microstructure and creep strength of near- α Ti alloy with a bimodal microstructure comprising lamellae and equiaxed α phase, which is practically important in high-temperature applications, are investigated. The Al equivalent values were set to be constant and no greater than 9 to suppress ordering or α_2 precipitation in the α phase.

Notably, the amounts of such α stabilizers affect other properties such as oxidation resistance, which is an important high-temperature property. From the perspective of designing a new high-temperature alloy, the effect of Ga, which is a solid solution strengthener, on the alloy's oxidation resistance is of practical interest. The oxidation mechanism of α - and α - β -Ti alloys has been previously studied (see, for example, References 19 through 22). In the oxidation process of near- α Ti alloys, external Al₂O₃ and internal TiO₂ form on the surface; the oxidation kinetics are essentially dominated by TiO₂ formation.^[21] Sn degrades the oxidation resistance, forming a metallic layer at the oxide/substrate interface^[23]; this metallic layer could deteriorate the adherence of oxides on surface. However, the literature contains few studies on the effect of Ga on the oxidation resistance of Ti alloys. In this study, the effect of Sn and/or Ga additions on the oxidation resistance of near- α Ti alloys was investigated and discussed.

II. EXPERIMENTAL PROCEDURE

Ingots (1.1 kg) of near- α Ti alloys—TKT8 with added Sn, TKT9 with added Sn and Ga, and TKT10 with added Ga—were produced by the cold crucible levitation melting method. All the alloys were double melted to enhance the uniformity of the ingot composition. The cast ingots were β -forged at 1373 K (1100 °C) and then groove rolled to 50 pct reduction at 1233 K (960 °C) in the $\alpha + \beta$ region to form square rods with sides of 14 mm. The alloys were heat treated at 1223 K (950 °C) for 1 h and then air cooled. Subsequently, they were aged at 863 K (590 °C) for 8 hours and air cooled.

The nominal chemical compositions of these alloys are shown in Table I. As previously mentioned, the

compositions were determined to be an almost constant value in terms of Al equivalence, although the Al-equivalence value was less than 9 to suppress the formation of the α_2 phase. The Al-equivalence values for TKT8, TKT9, and TKT10 were 8.63, 8.3, and 8.3, respectively. The Al-equivalence values for Sn and Ga in TKT9 were 1.01 and 0.99, respectively.

To investigate the oxidation behavior of unalloyed α -Ti and α -Ti with added Ga or Sn, unalloyed α -Ti, Ti-5.72 wt pct Ga (Ti-4.0 at. pct Ga), and Ti-9.37 wt pct Sn (Ti-4.0 at. pct Sn) were also cast by the cold crucible levitation melting method. These metals were forged at 1373 K (1100 °C) and then groove rolled to 50 pct reduction at 1373 K (1100 °C) to form square rods with 14 mm sides. The rods were subsequently aged at 973 K (700 °C) for 4 hours and then air cooled. The specimens for the creep tests and oxidation tests were machined from the heat-treated bars. The dimensions of the creep specimens were as follows: 6 mm gage diameter and 30 mm gage length, which conforms to Japanese Industrial Standard (JIS) Z 2201. The creep test was conducted at 873 K (600 °C) and 923 K (650 °C) under 310 MPa in air according to JIS Z 2271. The specimens for the oxidation tests were 8 mm in diameter and 4 mm in height, and the surfaces of the specimens were polished using #800 grit SiC paper, followed by ultrasonic cleaning in acetone. Isothermal oxidation tests were performed at 973 K and 1023 K (700 °C and 750 °C) in laboratory air for the alloys shown in Table I and at 973 K (700 °C) for α -Ti, Ti-9.37 wt pct Sn, and Ti-5.72 wt pct Ga. The samples in alumina crucibles were removed from the furnace after 20, 45, 70, 90, 110, 140, and 240 h at 750 °C and after 340 hours at 973 K (700 °C). The mass change of each sample was measured using a microbalance with a precision of ± 0.0001 g. Before microstructural characterization, the samples were metallographically polished using conventional techniques. The microstructures of the samples were analyzed using field-emission-gun scanning electron microscopy (FEG-SEM; JEOL JSM 7001F). Chemical analyses were performed using energy-dispersive X-ray spectroscopy (EDS); the EDS apparatus was attached to the electron microscope. The constituent oxide phases were identified by X-ray diffractometry (XRD). The volume fraction of the primary α phases in the alloy microstructures was determined using the point-count method according to standard ASTM E562.

III. RESULTS AND DISCUSSION

After heat treatment at 863 K (590 °C), the microstructures of TKT8 with added Sn, TKT9 with

Table I. Chemical Compositions (Wt Pct) of TKT8, TKT9, and TKT10. Ti Content Balanced (Wt Pct). Volume Fraction (VF) of the Primary Equiaxed α Phase, Al Equivalence in TKT8, TKT9, and TKT10

Alloy	Al	Sn	Ga	Zr	Mo	O	Al Eq.	VF
TKT8	4.91	5.99	—	3.95	0.99	0.067	8.63	14.3
TKT9	4.92	3.04	1.98	3.96	1.01	0.072	8.30	38.8
TKT10	4.91	—	3.99	3.95	1.03	0.074	8.30	44.5

added Sn and Ga, and TKT10 with added Ga, which are perpendicular to the rolling directions, are bimodal structures comprising α - β -lamellae and equiaxed α phase, as shown in Figure 1. The volume fraction of equiaxed α phase increased because of the replacement of Sn with Ga, *i.e.*, 14.3 pct for TKT8, 38.8 pct for TKT9, 44.5 pct for TKT10, respectively, as shown in Table I. This increase in the volume fraction of equiaxed α phase is associated with an increase in the β -transus temperature, which is a consequence of the high volume fraction of α phase at 1223 K (950 °C) for heat treatment. The ascription of the increase in the β -transus temperature due to the replacement of Sn with Ga is supported by the temperature change of the α - β phase transition in binary systems. In the binary Ti-Ga system, the addition of Ga to Ti to a concentration of approximately 13.5 at. pct (18.5 wt pct) results in an increase in the α - β phase transition temperature^[24]; in contrast, the addition of Sn to Ti to concentrations of approximately 6.5 at. pct (14.7 wt pct) effectively decreases the α - β phase transition temperature.^[25] Thus, the volume fraction of the equiaxed α phase clearly depends on the alloy chemical composition, even when the Al-equivalence values among the near- α alloys are nearly equal. Notably, the difference in the volume fraction of equiaxed α phase between TKT9 and TKT10 (5.7 pct) is less than 24.5 pct of that between TKT8 and TKT9, which indicates a stronger effect of the Sn on the microstructure.

Sn and Ga are solid solution strengtheners of α -Ti at room temperature and at high temperatures, respectively. The Sn-added α -Ti exhibited greater tensile strength than the Ga-added α -Ti at high temperatures when the atomic fractions of Sn and Ga were equal.^[6] However, according to the tensile strengths of unalloyed α -Ti, Ti-5.72 wt pct Ga (Ti-4.0 at. pct Ga), and Ti-9.37 wt pct Sn (Ti-4.0 at. pct Sn) at 923 K (650 °C),^[17] the addition of 9.37 wt pct Sn increased the tensile strength by 103 MPa at 923 K (650 °C), whereas the addition of 5.72 wt pct Ga increased it by 121 MPa. Ga was thus more effective than Sn in increasing the tensile strength at 923 K (650 °C) at the same quantity per unit weight.^[17] Literature contains no reports involving a comparison of the creep strength of Sn- and Ga-containing α -Ti alloys. In this study, the replacement of Sn with Ga affects the solid solution strengthening in the α and β phases and the microstructure morphology. Our

EDS results suggest that Ga preferentially partitioned into the α phase to a greater extent than Sn, as shown in Table II. However, the concentrations of Al, Zr, and Mo in the equiaxed α phase were very similar among TKT8, TKT9, and TKT10. The α phase composition affects the creep process, which is regarded as a thermally activated process that includes dislocation climb, where the mobility of a solute atom in alloyed α -Ti can vary with the solute atom's effective size.^[7,18,26]

The tensile strength at 923 K (650 °C) suggests that the α phase in the Ga-added alloy may lead to a higher creep strength than that in the Sn-added alloy. However, the creep behavior was strongly dependent on the microstructure morphology in this study, as shown in the creep curves collected at 873 K (600 °C) and 923 K (650 °C) under a constant stress of 310 MPa (Figure 2). TKT8 with 14.3 pct equiaxed α phase exhibited the highest creep rupture life at both temperatures, followed by TKT 9 and TKT10, with 38.8 pct and 44.5 pct equiaxed α phase, respectively. The difference in creep rupture life between TKT8 and TKT9 is 4.3 times greater than that between TKT9 and TKT10 at 873 K (600 °C) and 6.8 times greater than that between TKT9 and TKT10 at 923 K (650 °C).

The steady-state creep rate of TKT8, TKT9, and TKT10 at 923 K (650 °C) increases almost linearly with the volume fraction of equiaxed α phase, as shown in Figure 3(a). However, at 873 K (600 °C), the steady-state creep rate increased more at high volume fractions of the equiaxed α phase. The presence of the lamellar structure is well known to increase creep resistance, whereas the equiaxed α structure increases fatigue resistance. With respect to creep, the primary creep rate and steady-state creep rate correlate well with the volume fraction of the equiaxed α phase in Ti-6242S and IMI 834 Ti alloys.^[27-30] In the case of Ti-6242S alloy, the creep strain and steady-state creep rate have

Table II. Chemical Composition (Wt Pct) of the Primary Equiaxed α Phase in TKT8, TKT9, and TKT10. Ti Content Balanced (Wt Pct)

Alloy	Al	Sn	Ga	Zr	Mo
TKT8	4.8	6.4	—	3.3	0.1
TKT9	4.8	3.1	2.9	3.3	0.1
TKT10	4.7	—	5.4	3.3	0.1

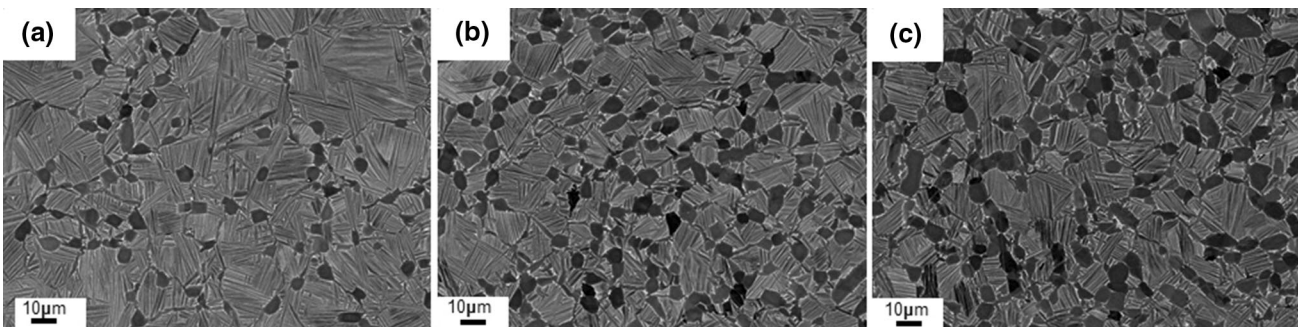


Fig. 1—Backscattered electron images and transmission electron images of heat-treated alloys (a) TKT8, (b) TKT9, and (c) TKT10.

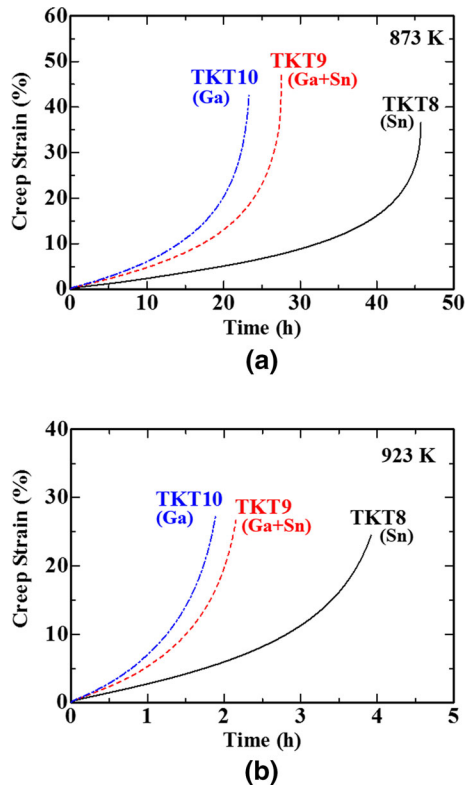


Fig. 2—Creep curves of TKT8, TKT9, and TKT10 under a constant stress of 310 MPa at (a) 873 K (600 °C) and (b) 923 K (650 °C).

been reported to be approximately the same at equiaxed α phase contents up to 30 pct; in addition, an increase in the equiaxed α phase volume fraction from 30 to 53 pct resulted in a large increase in creep at 783 K (510 °C) and 241 MPa.^[28] In contrast, IMI 834 has been reported to exhibit an almost linear increase in minimum creep rate at equiaxed α phase contents up to 70 pct at 923 K (650 °C) and 220 MPa.^[30] Similarly, in this study, the creep behavior varied with the microstructure although the effects of the amounts of Sn and Ga on the creep properties were considered, as previously discussed. We assumed that the creep behavior can be characterized by

$$\dot{\epsilon} = K(\sigma)^n \exp(-Q_{app}/RT)$$

where $\dot{\epsilon}$ is the steady-state creep rate, K and n are constants, σ is the applied stress, Q_{app} is the apparent activation energy, R is the gas constant, and T is absolute temperature. This equation can be rewritten as $\ln \dot{\epsilon} = \ln K + n \ln \sigma - Q_{app}/RT$.

The apparent activation energy for the steady-state creep rate was determined from temperature-change tests in the secondary creep stage using the Arrhenius plots as shown in Figure 3(b), *i.e.*, 338 kJ/mol for TKT8, 342 kJ/mol for TKT9, and 314 kJ/mol for TKT10. Bania and Hall demonstrated that a full lamellar structure was superior to a bimodal microstructure with respect to the creep rate in Ti-6242S, as previously mentioned.^[27] In their study, the activation energy for full lamellae (372 kJ/mol) was lower than that (418 kJ/mol) for the bimodal microstructure with 19 pct

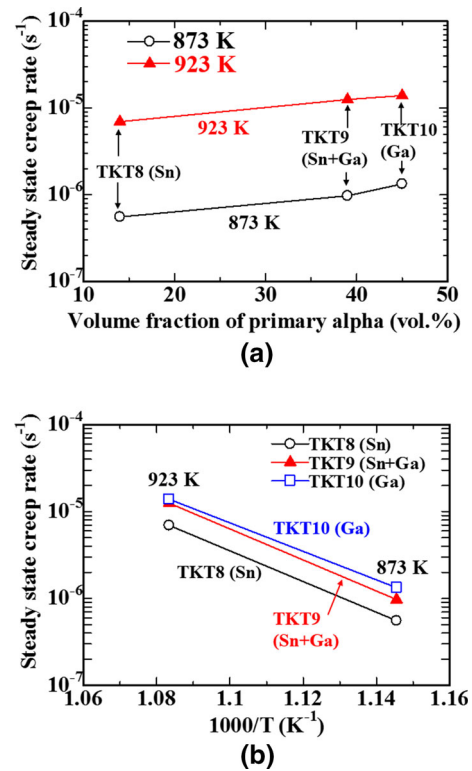


Fig. 3—Steady-state creep rate as a function of the volume fraction of primary α phase (a). Arrhenius plots of the temperature dependence of the steady-state creep rates of TKT8, TKT9, and TKT10 (b).

equiaxed α phase in the temperature range between 742 K and 838 K (496 °C and 565 °C) at 345 MPa. The results of the present study revealed an opposite tendency with respect to the microstructure effect; specifically, the activation energy of TKT8, which contained a smaller volume fraction of equiaxed α phase, was greater than the activation energy of TKT10 in the temperature range between 873 K and 923 K (600 °C and 650 °C) at 310 MPa. In addition, the difference in the volume fraction of equiaxed α phase between TKT9 and TKT10 was small. Those results indicate that the replacement of Sn with Ga decreased the activation energy of the steady-state creep rate.

Creep behaviors that differ depending on the microstructure morphology have been previously discussed by other authors.^[27–35] The superior creep strength with the small volume fraction of equiaxed α phase in the present study is attributed to the concomitant effect of the following factors: (1) a larger colony size and prior β -grain size with a large volume of lamellar structure, which determines the dislocation-gliding distance; (2) possibly less grain-boundary sliding^[34,35]; and (3) an increase in the strength of the lamellar matrix in the bimodal structure as a consequence of alloy-element partitioning.^[29] In the case of higher activation energies, the rate-controlling process at higher temperatures was assumed to be diffusion controlled because the activation energy for the high-temperature creep was similar to that of self-diffusion in α -Ti (*e.g.*, 242 kJ/mol).^[26] Therefore, we

concluded that deformation in the α phase is dominant in near- α Ti alloys with a small volume fraction of β phase, even though the activation energy in α -Ti is affected by solute diffusion.^[36] The activation energies obtained in this study are greater than that for self-diffusion in α -Ti and are similar to the values reported for conventional alloys such as Ti-6242S and IMI 834,^[27,32,33] even though the effects of Si solid solution and silicide precipitation were not factors in this study.

Figure 4 shows the mass gain per unit area of the alloys oxidized in air for 340 hours at 973 K (700 °C) (a) and for 240 hours at 1023 K (750 °C) (b). The overall mass gains of TKT8, TKT9, and TKT10 were 1.75, 1.65, 1.48 mg/cm², respectively, after oxidation for 340 hours at 973 K (700 °C). The difference in the mass gains among TKT8, TKT9, and TKT10 was not substantial. Slight spallation of oxides on the surface of TKT8 was observed after the oxidation test at 973 K (700 °C), as shown in Figure 5(a). The increase in Ga content clearly suppressed the spallation of the oxides. At 1023 K (750 °C), the oxidation for all the alloys was accelerated and the oxide scales spalled more extensively, as shown in Figures 5(d), (e), and (f). Sn-bearing TKT8 shows a sudden decrease in mass gain in Figure 4b; this decrease is attributed to oxide spallation.

The mass gain during oxidation is well known to depend on oxide formation and oxygen dissolution.^[37] This oxygen dissolution is affected by the microstructure. Leyens *et al.* suggested on the basis of the substantial grain boundary/grain ratio in IMI 834 and TIMETAL 1100 alloys that oxygen diffusion is faster in a bimodal microstructure than in a lamellar structure.^[20]

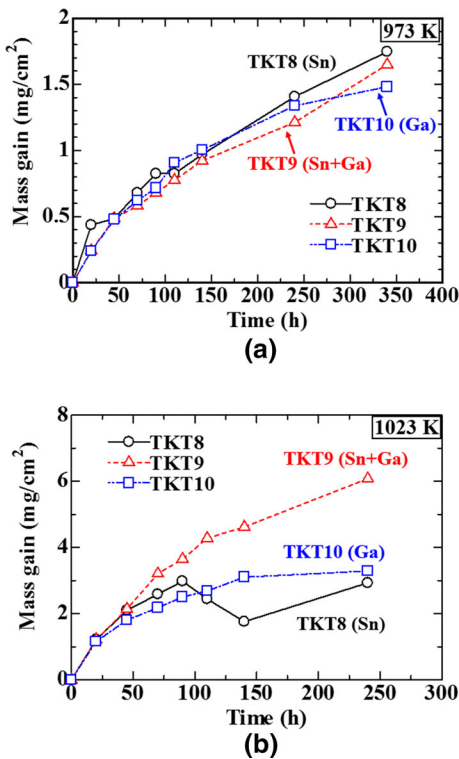


Fig. 4—Mass gains for specimens of TKT8, TKT9, and TKT10 oxidized at (a) 973 K (700 °C) and (b) 1023 K (750 °C).

However, this effect was not significant compared to that of oxide growth, and it was assumed to represent a small contribution.^[20] In the present study, the microstructure of all the alloys are bimodal, with equiaxed α and lamellar ($\alpha + \beta$) structures, where the volume fraction of the equiaxed α phase varies. The difference in oxygen dissolution in the present microstructures may be smaller than that in the aforementioned work, where a bimodal microstructure was compared with the full lamellar structure.

Figure 6 shows the XRD patterns of TKT8, TKT9, and TKT10 oxidized at 973 K and 1023 K (700 °C and 750 °C). TiO₂ (rutile) and α -Al₂O₃ were observed on the surfaces of all the alloys. At 1023 K (750 °C), (GaAl)₂TiO₅ was also confirmed on the surface. The peak for α -Ti was also detected because of the penetration of the X-rays through the oxide scales. The intensity ratios of TiO₂/Al₂O₃ for TKT8, TKT9, and TKT10 oxidized at 973 K (700 °C) were 0.40, 0.35, and 0.14, respectively. This intensity ratio decreased with the amount of Sn, which means that the replacement of Sn with Ga suppressed TiO₂ formation or promoted Al₂O₃ growth.

Sn addition to unalloyed α -Ti has been reported to promote TiO₂ formation on the metal surface, and Sn segregates as a metallic layer at the interface between the oxide and substrate.^[23] These behaviors are thought to occur because of vacancies created by the diffusion of Sn to the interface; these vacancies facilitate the diffusion of Ti, thereby enhancing the formation of TiO₂.^[23]

Figure 7 shows the elemental concentration profiles of Ti, Al, Sn, Ga, and O in the oxide layers and in the substrates of TKT8 (a), TKT9 (b), and TKT10 oxidized at 973 K (700 °C) (c) and TKT10 oxidized at 1023 K (750 °C) (d), where the profiles were obtained along the lines in Figure 8. Sn segregated in the substrate near the TiO₂/substrate interface, as shown in Figures 7(a) and (b); this segregation can deteriorate the adherence of oxides at the interface, as reported for Sn-added α -Ti and α - β alloys.^[22,23] For all the alloys oxidized at 973 K (700 °C), TiO₂ formed internally and Al was enriched at the external Al₂O₃ layer. Several Al peaks were observed in the TiO₂ regions of the concentration profiles of Sn-added TKT8 and TKT9 in Figure 7, indicating the formation of alternating layers of Al₂O₃ and TiO₂.

With respect to the oxidation behavior in an α - β alloy, multilayered oxides comprising alternating layers of Al₂O₃ and TiO₂ reportedly formed in Ti-6Al-4V during oxidation.^[19] The external gas/oxide interface was always occupied by Al₂O₃, although Al₂O₃ formed on an alloy containing less than 50 at. pct Al is not a protective, continuous layer.^[38,39] The external formation of Al₂O₃ and the internal formation of TiO₂ were observed in this study, consistent with the results of previous studies.^[20,22] Clearly, oxide formation on Ga-added TKT10 was suppressed: the oxide thickness reached 3.5 μ m, which is approximately half of the 8 μ m thickness observed in the cases of both TKT8 and TKT9, although the mass gains were similar, as previously mentioned. This thinner oxide layer could be due to the differences in density among Al₂O₃, TiO₂, and Ga₂O₃. Ga dissolved uniformly in TiO₂ and Al₂O₃ in

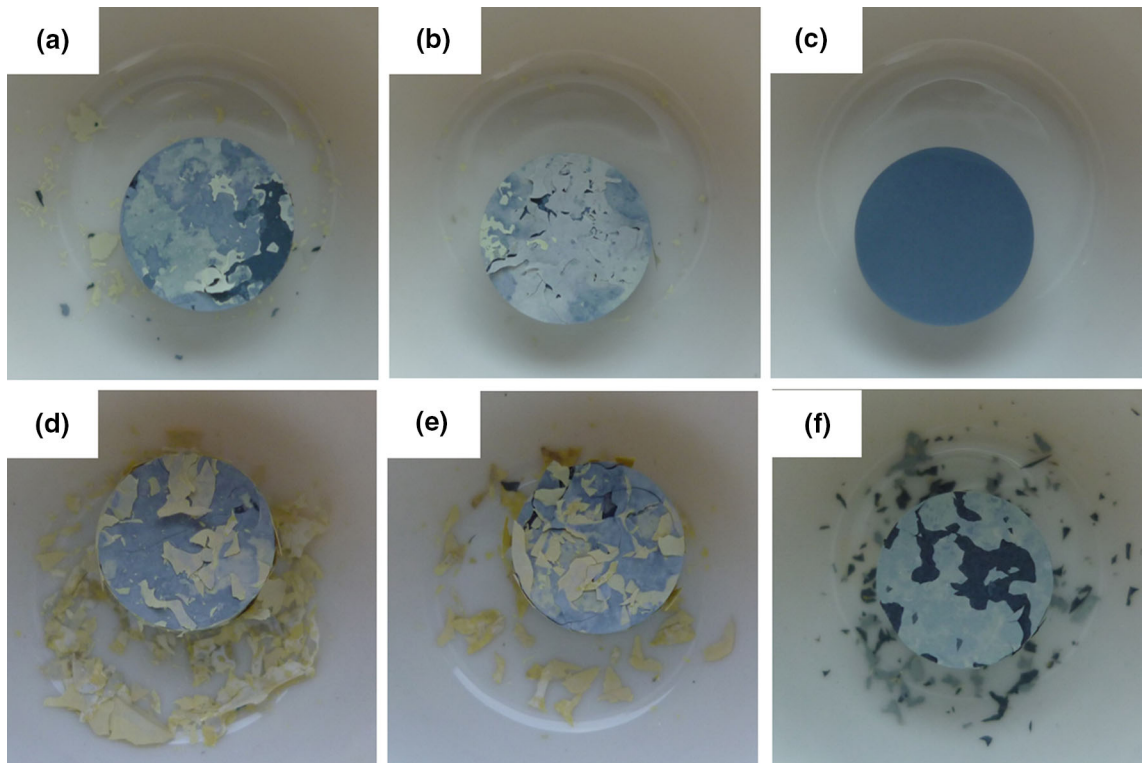


Fig. 5—Surfaces of (a, d) TKT8, (b, e) TKT9, and (c, f) TKT10 in crucibles; these samples were oxidation tested at (a to c) 973 K (700 °C) or (d to f) 1023 K (750 °C).

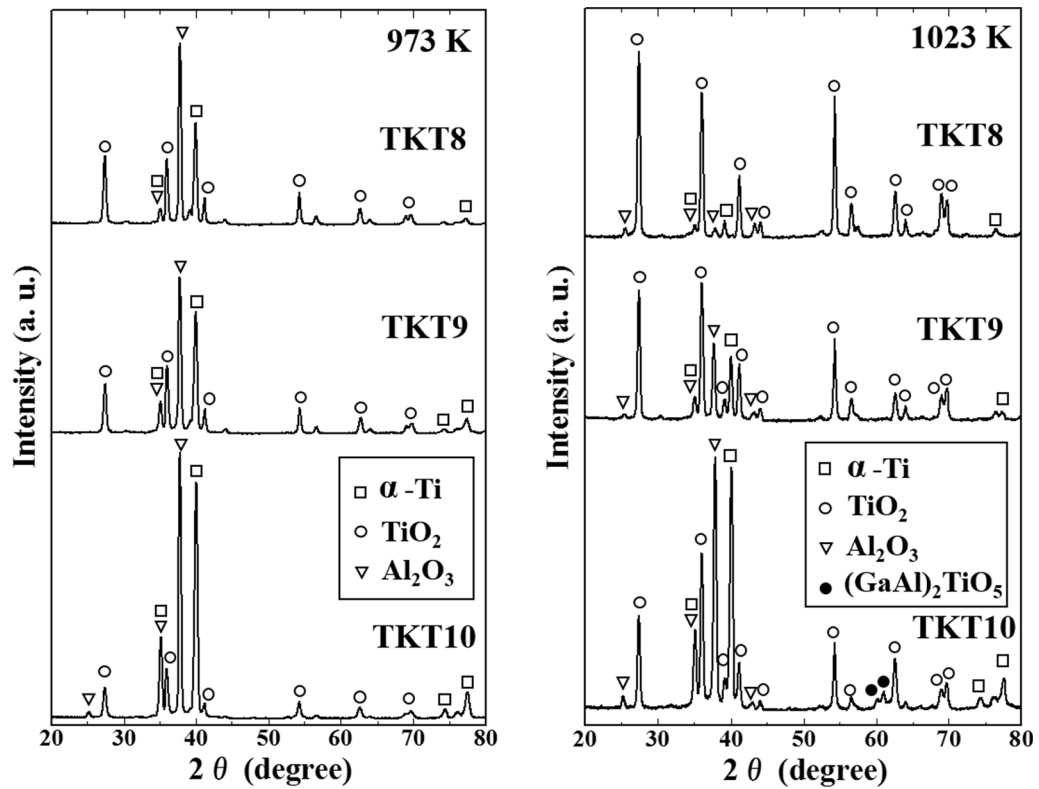
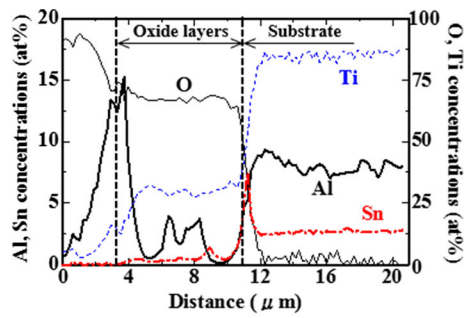
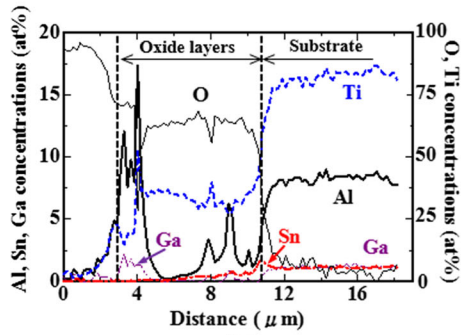


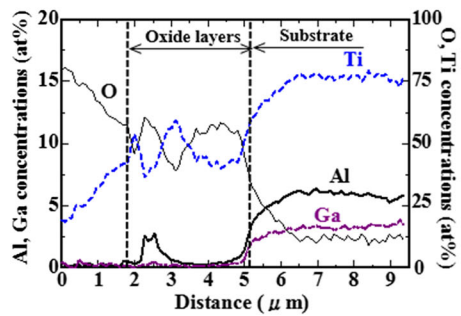
Fig. 6—XRD patterns of TKT8, TKT9, and TKT10 oxidized at 973 K and 1023 K (700 °C and 750 °C).



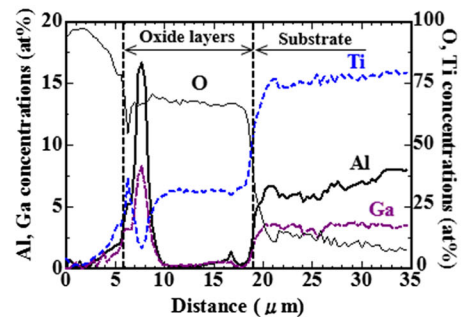
(a)



(b)

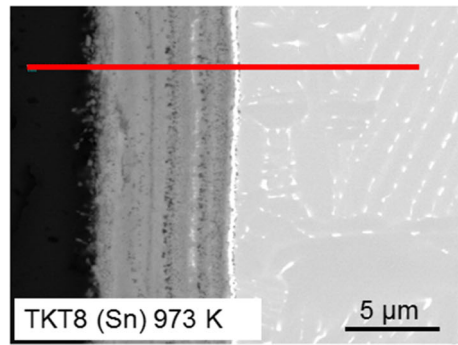


(c)

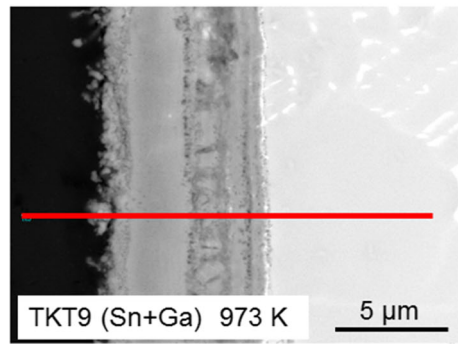


(d)

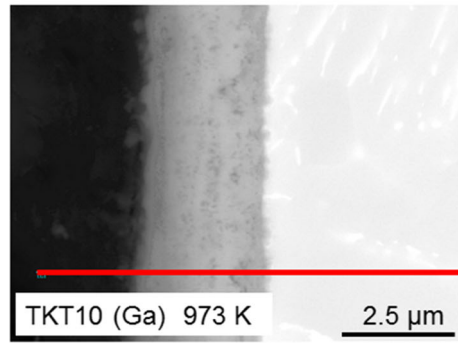
Fig. 7—Concentration profiles for TKT8 (a), TKT9 (b), and TKT10 (c) oxidized at 973 K (700 °C) and TKT10 (d) oxidized at 1023 K (750 °C). These profiles were obtained in the oxide layers and the substrate along the lines in Fig. 8.



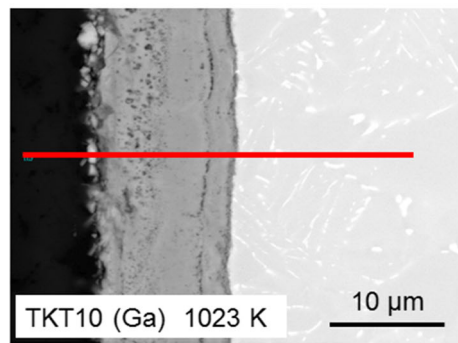
(a)



(b)



(c)



(d)

Fig. 8—Backscattered electron image of the oxide layers and the substrates in TKT8 (a), TKT9 (b), and TKT10 (c) oxidized at 973 K (700 °C) and TKT10 (d) oxidized at 1023 K (750 °C).

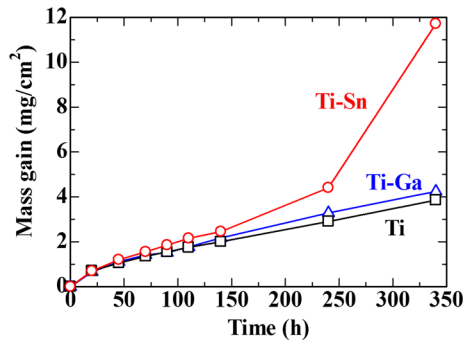


Fig. 9—Mass gain vs time for unalloyed α -Ti, Ti-9.37 wt pct Sn, and Ti-5.72 wt pct Ga, all of which were oxidized at 973 K (700 °C) for 340 h.

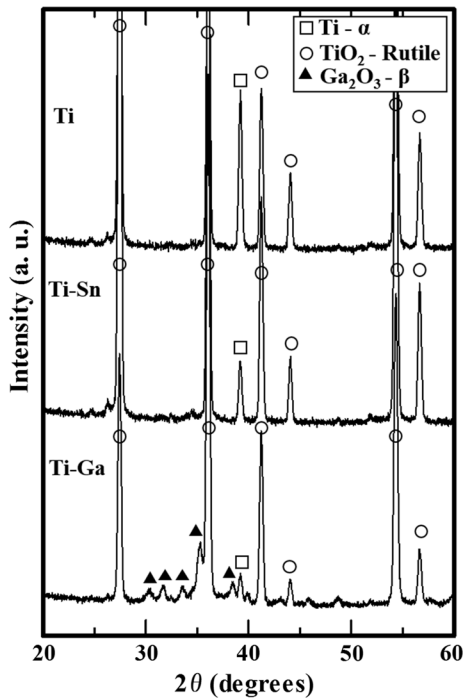


Fig. 10—XRD patterns of unalloyed α -Ti, Ti-9.37 wt pct Sn, and Ti-5.72 wt pct Ga, all of which were oxidized at 973 K (700 °C).

TKT10 without Ga segregation at the TiO_2 /substrate interface during oxidation, as shown in Figure 7(c). In contrast, Ga was enriched in the external Al_2O_3 layer and in an Al-rich layer in TiO_2 in TKT9, as shown in Figure 7(b), where the oxidation was more accelerated than in the case of TKT10.

To the best of our knowledge, there have been no studies of the effect of Ga on the oxidation behavior of α and α - β Ti alloys. To discuss the effect of Ga, we investigated the formation of Ga_2O_3 on α -Ti. Figure 9 shows the mass gain per unit area of unalloyed α -Ti and Ti-5.72 wt pct Ga (Ti-4.0 at. pct Ga) oxidized in air at 973 K (700 °C). The result of Ti-9.37 wt pct Sn (Ti-4.0 at. pct Sn) was also given to show the accelerated formation of TiO_2 in Sn-added Ti. The overall mass gains after oxidation for 340 hours at 973 K (700 °C)

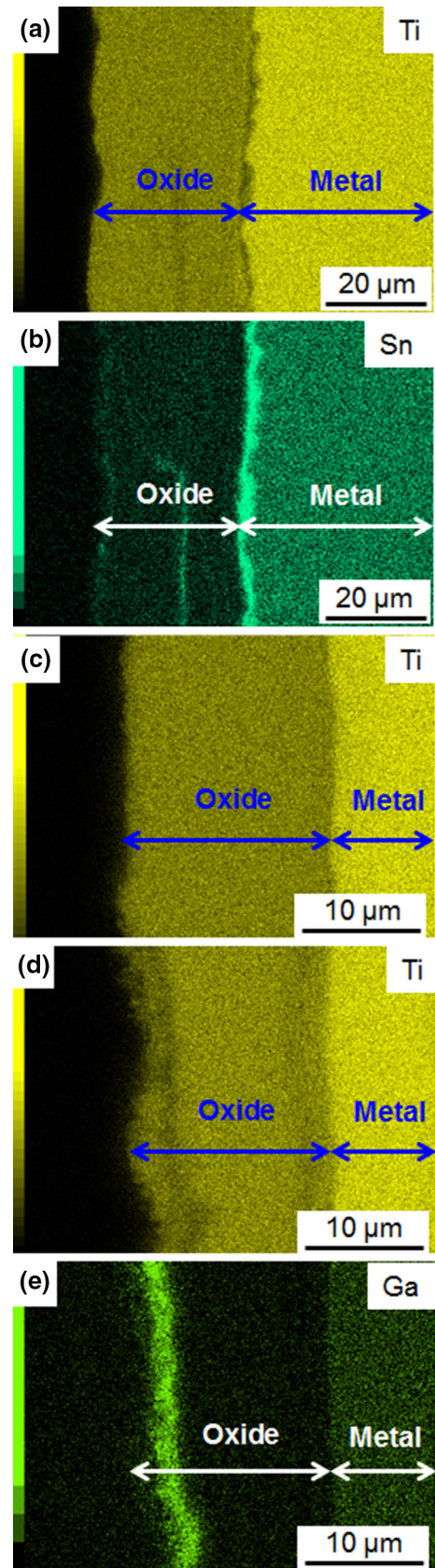


Fig. 11—Elemental mapping images of the oxide layers and the substrate metal in Ti-9.37 wt pct Sn (a to b) alloy, unalloyed Ti (c), and Ti-5.72 wt pct Ga (d to e).

were 3.85 mg/cm² for unalloyed Ti, 4.24 mg/cm² for Ti-5.72 wt pct Ga, and 11.71 mg/cm² for Ti-9.37 wt pct Sn. Ga-added Ti exhibited a mass gain similar to that observed for unalloyed Ti, forming β -Ga₂O₃ and TiO₂, as shown in the XRD patterns in Figure 10.

The elemental mapping image shown in Figure 11 indicates that, in the case of Ga-added Ti, the thickness of the oxide layers (including the external Ga₂O₃ layer) formed on the substrate were similar between unalloyed Ti and Ti-5.72 wt pct Ga. Thus, no significant difference was observed in the mass gain and the oxide thickness between unalloyed Ti and Ti-5.72 wt pct Ga. The oxide growth in TKT10 may be suppressed primarily by the formation of a solid solution of Al₂O₃ and Ga₂O₃. The thickness of oxides on unalloyed Ti and Ti-5.72 wt pct Ga (approximately 18 μ m) was smaller than that on Ti-9.37 wt pct Sn (approximately 31 μ m), with Sn segregation at the TiO₂/substrate interface in the metal. The growth of Ga₂O₃ may not be preferential in α -Ti alloy because of the Ga concentration at the interface; the Gibbs free energies of oxide formation according to Ellingham diagrams are -530 kJ/mol for Ga₂O₃, -660 kJ/mol for TiO₂, and -830 kJ/mol for Al₂O₃ at 1000 K (727 °C).^[40] The pure components of Al₂O₃ and Ga₂O₃ are stable phases in air from their melting points to room temperature.^[41] In addition, according to the phase relationship in the Ga₂O₃-Al₂O₃-TiO₂ system at 1673 K (1400 °C), a continuous solid solution exists between Ga₂TiO₅ and Al₂TiO₅.^[42] A two-phase field of Al₂O₃ and (GaAl)₂TiO₅ exists near the Al₂O₃-rich side in the system. In this study, the XRD peak of (GaAl)₂TiO₅ was detected on the surface of TKT10 oxidized at 1023 K (750 °C), as shown in Figure 6. (GaAl)₂TiO₅ may have formed near or in Al₂O₃ on the surface, although the location of (GaAl)₂TiO₅ in oxides could not be identified.

The diffusivity of elements, including oxygen in Ga₂O₃ and (GaAl)₂TiO₅, is not clear at this time, although Al₂O₃ is known to act as a barrier that modifies the oxygen flux across oxide layers, which results in a decrease in the oxidation rate.^[43] We concluded that the replacement of Sn with Ga suppressed oxide growth and improved the adherence of oxides in α - β -Ti alloys, without Ga segregation at the TiO₂/substrate interface in the ranges of composition and temperature investigated in this study. As previously discussed, Ga addition increases the high-temperature tensile strength and creep strength, although the control of the microstructure morphology is necessary. In the future, Ga addition to near- α alloys could enable the development of high-temperature Ga-bearing near- α alloys with good high-temperature strength and high oxidation resistance, enabling the amount of Sn, which enhances TiO₂ growth and the spallation of oxides, to be reduced.

IV. CONCLUSIONS

The creep and oxidation behaviors of Ga- and/or Sn-bearing near- α Ti alloys based on Ti-5Al-4Zr-1Mo with a bimodal structure were investigated. The

amounts of Sn and Ga were set to be approximately constant with respect to Al equivalent. The results of the present study led to the following conclusions:

- (1) The replacement of Sn with Ga increased the volume fraction of equiaxed α phase because of the increase in β transus temperature. An α stabilizer, Ga, preferentially partitioned into the α phase to a greater extent than Sn.
- (2) The creep strain rate was strongly dependent on the volume fraction of equiaxed α phase. The replacement of Sn with Ga led to smaller apparent activation energies for the steady-state creep rate.
- (3) Ga suppressed oxide growth and the spallation of oxide scales in the near- α alloys. Ga₂O₃ dissolved in TiO₂ and Al₂O₃ without Ga segregation at the TiO₂/substrate interface. In contrast, Sn-added alloys exhibited degraded oxidation resistance, which promoted TiO₂ formation, Sn segregation at the interface, and oxide spallation.

REFERENCES

1. G. Lütjering and J.C. Williams: *Titanium*, 2nd ed., Springer, Berlin, 2003.
2. S. Saal, L. Wagner, G. Lütjering, H. Pillhöfer, and M.A. Daeubler: *Z. Metallkde.*, 1990, vol. 90, pp. 535-39.
3. D.F. Neal, S.P. Fox: in *Titanium '92, Science and Technology*, F.H. Froes and I.L. Caplan, eds., TMS, PA, 1993, pp. 287-94.
4. C. Ramachandra, A.K. Singh, and G.M.K. Sarma: *Met. Trans. A*, 1993, vol. 24, pp. 1273-80.
5. H. Sasano, H. Kimura: in *Titanium '80, Science and Technology*, H. Kimura and O. Izumi, eds., Metallurgical Society of AIME, PA, 1980, pp. 1147-54.
6. H. Conrad, M. Doner, B. de Meester: *Titanium Science and Technology*, R.I. Jaffee and H.M. Burte, eds., Plenum Press, NY, 1973, pp. 969-1005.
7. H.L. Gegel, S. Fujishiro: *Titanium Science and Technology*, R.I. Jaffee and H.M. Burte, eds., Plenum Press, NY, 1973, pp. 2179-94.
8. M. Hoch, T. Sakai, J.J. Krupowicz, M. Delahanty: in *Titanium Science and Technology*, R.I. Jaffee and H.M. Burte, eds., Plenum Press, NY, 1973, pp. 935-49.
9. G. Lütjering and S. Weissmann: *Acta Met.*, 1970, vol. 18, pp. 785-95.
10. M.J. Godden, W.N. Roberts: *Titanium Science and Technology*, R.I. Jaffee and H.M. Burte, eds., Plenum Press, NY, 1973, pp. 2207-18.
11. J.C. Williams, M.J. Blackburn: in *Ordered Alloys*, H. Kear, T. Sims, S. Stoloff, and J. H. Westbrook, eds., Claitor's Publishing Division, Baton Rouge, LA, 1970, pp. 425-45.
12. H.W. Rosenberg: in *The Science, Technology and Application of Titanium*, R.I. Jaffee and N.E. Promisel, eds., Pergamon Press, Oxford, 1970, pp. 851-59.
13. C.E. Shamblen and T.K. Redden: *Met. Trans.*, 1972, vol. 3, pp. 1299-1305.
14. P.G. Partridge: *Met. Rev.*, 1967, vol. 12, pp. 169-94.
15. N.E. Paton and W.A. Backofen: *Met. Trans.*, 1970, vol. 1, pp. 2839-47.
16. J.C. Williams, R.G. Baggerly, and N.E. Paton: *Metall. Mater. Trans. A*, 2002, vol. 33A, pp. 837-50.
17. T. Kitashima, Y. Yamabe-Mitarai, S. Iwasaki, and S. Kuroda: *Proceeding of The 13th World Conference on Titanium (Ti-2015)* (in press).
18. K.S. Jepson, L. Lark, C.A. Stubbington: in *The Science, Technology and Application of Titanium*, R.I. Jaffee and N.E. Promisel, eds., Pergamon Press, Oxford, 1970, pp. 861-73.
19. H.L. Du, P.K. Datta, D.B. Lewis, and J.S. Burnell-Gray: *Corros. Sci.*, 1994, vol. 36, pp. 631-42.

20. C. Leyens, M. Peter, and W.A. Kaysser: *Mater. Sci. Technol.*, 1996, vol. 12, pp. 213–18.
21. C. Leyens, M. Peter, and W.A. Kaysser: *Mater. Sci. Forum*, 1997, vols. 251–254, pp. 769–76.
22. T. Kitashima and Y. Yamabe-Mitarai: *Metall. Mater. Trans. A*, 2015, vol. 46A, pp. 2758–67.
23. E.M. Kenina, I.I. Kornilov, and V.V. Vanilova: *Met. Sci. Heat Treat.*, 1972, vol. 14, pp. 396–98.
24. J.L. Murray: *Bull. Alloy Phase Diagrams*, 1985, vol. 6, pp. 327–30.
25. J.L. Murray: in *Phase Diagrams of Binary Titanium Alloys*, J.L. Murray, ed., ASM International, Metals Park, OH, 1987, pp. 294–99.
26. M. Doner and H. Conrad: *Met. Trans.*, 1973, vol. 4, pp. 2809–17.
27. P.J. Bania, J.A. Hall: in *Titanium '84, Science and Technology*, G. Lütjering, U. Zwicker, and W. Bunt, eds., DGM, Oberursel, 1985, pp. 2371–78.
28. K.E. Thieshen, M.E. Kassner, J. Pollard, D.R. Hiatt, and B.M. Bristow: *Met. Trans. A*, 1993, vol. 24, pp. 1819–26.
29. C. Andres, A. Gysler, and G. Lütjering: *Z. Metallkde.*, 1997, vol. 88, pp. 197–203.
30. H. Mishra, P. Ghosal, T.K. Nandy, and P.K. Sagar: *Mater. Sci. Eng. A*, 2005, vol. 597, pp. 222–31.
31. W.H. Miller, Jr., R.T. Chen, E.A. Starke, Jr.: *Met. Trans. A*, 1987, vol. 18, pp. 1451–68.
32. M. Es-Souni: *Metall. Mater. Trans. A*, 2001, vol. 32A, pp. 285–93.
33. R.W. Hayes, G.B. Viswanathan, and M.J. Hills: *Acta Mater.*, 2002, vol. 50, pp. 4953–63.
34. N.E. Paton and M.W. Mahoney: *Met. Trans. A*, 1976, vol. 7, pp. 1685–94.
35. S. Ankem and H. Margolin: *Met. Trans. A*, 1983, vol. 14, pp. 500–03.
36. M. Koppers, C. Herzig, M. Friesel, and Y. Mishin: *Acta Mater.*, 1997, vol. 45, pp. 4181–91.
37. T. Kitashima, L.J. Liu, and H. Murakami: *J. Electrochem. Soc.*, 2013, vol. 160, pp. C441–44.
38. S. Becker, A. Rahmel, M. Schorr, and M. Schütze: *Oxid. Met.*, 1992, vol. 38, pp. 425–64.
39. K.L. Luthra: *Oxid. Met.*, 1992, vol. 38, pp. 475–90.
40. S. Desmoulin-Krawiec, C. Aymonier, A. Loppinet-Serani, F. Weill, S. Gorsse, J. Etourneau, and F. Cansell: *J. Mater. Chem.*, 2004, vol. 14, pp. 228–32.
41. V.G. Hill, R. Roy, and E.F. Osborn: *J. Am. Ceram. Soc.*, 1952, vol. 35, pp. 135–42.
42. A.L. Jaromin and D.D. Edwards: *J. Am. Ceram. Soc.*, 2005, vol. 88, pp. 2573–77.
43. A.M. Chaze and C. Coddet: *J. Less Common Met.*, 1990, vol. 157, pp. 55–70.